CHEMISTRY
A EUROPEAN JOURNAL

DOI: 10.1002/chem.200601643

# Breaking Chemistry's Strongest Bond: Can Three-Coordinate [M{N(R)Ar}$_3$] Complexes Cleave Carbon Monoxide?

**Gemma Christian,[a] Robert Stranger,*[a] Simon Petrie,[a] Brian F. Yates,[b] and Christopher C. Cummins[c]**

**Abstract:** The reaction pathway for the interaction of CO with three-coordinate $Ta^{III}$, $W^{III}$ and $Re^{III}$ complexes (modelled on the experimental [M{N-(*t*Bu)Ar}$_3$] system) has been explored by using density functional methods. Calculations show that CO binds without a barrier to [Re(NH$_2$)$_3$], forming the encounter complex [OC–Re-(NH$_2$)$_3$], which is stabilized by $\approx$280 kJ mol$^{-1}$ relative to the reactants. The binding of [Ta(NH$_2$)$_3$] to the oxygen terminus of CO is inhibited by a barrier of only 20 kJ mol$^{-1}$ and is followed by spontaneous cleavage of the C–O bond to form the products [C–Re(NH$_2$)$_3$] and [O–Ta(NH$_2$)$_3$]. The salient features of the potential energy surface are more favourable to CO cleavage than the analogous $N_2$ cleavage by [Mo(NH$_2$)$_3$], which is less exothermic (335 vs. 467 kJ mol$^{-1}$) and is impeded by a significant barrier (66 kJ mol$^{-1}$). The $Re^{III}$/$Ta^{III}$/CO system therefore appears to be an excellent candidate for cleaving the exceptionally strong C–O bond under mild laboratory conditions. The related $W^{III}$/$Ta^{III}$ dimer, which significantly weakens but does not cleave the CO bond, may be a suitable alternative when the chemistry is to be performed on activated CO rather than on the strongly bound oxide and carbide cleavage products.

**Keywords:** C–O activation · density functional calculations · rhenium · tantalum · three-coordinate complexes

## Introduction

One of chemistry's supreme ironies is that although carbon is the archetypal tetravalent element, its most abundant molecular form does not conform to this expected valence. The molecule in question, carbon monoxide, is also notable for possessing the strongest bond in chemistry: $D^{\circ}_{298}(C{\equiv}O) = (1076.4 \pm 0.7)$ kJ mol$^{-1}$, exceeding the value for isoelectronic $N_2$ by well over 100 kJ mol$^{-1}$. The extreme robustness of the carbon monoxide bond has many implications. In biochemistry, its stability results in a tendency to "poison" some metalloenzymes such as haemoglobin,[1,2] from which adsorbed CO is not readily removed or destroyed; conversely, CO also has important functions as a biochemical signalling molecule[3,4] and as a resource for microbial processing.[5] In industry, CO is a constituent of synthesis gas, serving as a feedstock for $H_2$ and $CH_4$ production through the water-gas shift (WGS) reaction[6] and Fischer–Tropsch catalysis.[7–9] Although CO also serves other uses,[10,11] for example, as a carbonylating agent in the conversion of alcohols to carboxylic acids, its role as a precursor to $H_2$ and hydrocarbons is dominant and can only increase in industrial and economic importance as subterranean hydrocarbon deposits are progressively depleted.[11]

One of the principal industrial uses for hydrogen produced through the WGS reaction is in the Haber–Bosch process of nitrogen fixation.[12,13] The latter shares with the WGS and Fischer–Tropsch reactions a requirement for high temperatures to drive the conversion of the strong, multiply bonded diatomics CO and $N_2$ into the desired products. The

[a] G. Christian, Prof. R. Stranger, Dr. S. Petrie
Department of Chemistry, Australian National University
Canberra, ACT 0200 (Australia)
Fax: (+61) 2-6125-0760
E-mail: Rob.Stranger@anu.edu.au

[b] Prof. B. F. Yates
School of Chemistry, University of Tasmania
Private Bag 75, Hobart, TAS 7001 (Australia)

[c] Prof. C. C. Cummins
Department of Chemistry, Massachusetts Institute of Technology
Cambridge, MA 02139 (USA)

Supporting information for this article is available on the WWW under http://www.chemeurj.org/ or from the author. It contains optimised structures, energies and spin states for [M(NH$_2$)$_3$], [OC–M-(NH$_2$)$_3$], [CO–M(NH$_2$)$_3$], [C–M(NH$_2$)$_3$] and [O–M(NH$_2$)$_3$] for M = $Re^{III}$ and $Ta^{III}$, and [(NH$_2$)$_3$M–CO–M′(NH$_2$)$_3$] for M, M′ = $Re^{III}$, $Ta^{III}$ and $Mo^{III}$. Linear transit data for 1) [M(NH$_2$)$_3$] + CO for M = $Re^{III}$ and $Ta^{III}$, 2) [OC–Re(NH$_2$)$_3$] + [Re(NH$_2$)$_3$] and 3) [C–Re-(NH$_2$)$_3$] + [O–Re(NH$_2$)$_3$].

contrast between the physical requirements for industrial versus biochemical fixation of nitrogen has spurred intensive research towards the development of catalysts and other agents that are better able to fix $N_2$ at modest temperatures and pressures.[14–18] A breakthrough in this field came with the discovery that sterically hindered three-coordinate complexes of molybdenum exhibit an ability to cleave $N_2$ at ambient pressure and modest temperatures. The mechanism for this reaction has been extensively studied through laboratory kinetic investigations[19,20] as well as through quantum chemical calculations.[21–23] N–N bond scission requires the successive end-on coordination of $N_2$ to $[Mo\{N(R)Ar\}_3]$ ($R = t$Bu, Ar = 3,5-$C_6H_3Me_2$), forming first the encounter complex $[N_2{-}Mo\{N(R)Ar\}_3]$ and second the intermediate dimer $[\{Ar(R)N\}_3Mo{-}NN{-}Mo\{N(R)Ar\}_3]$ (see Scheme 1). Traversal of an activation barrier then results in cleavage of the $N_2$ bond generating the nitrido product $[NMo\{N(R)Ar\}_3]$.

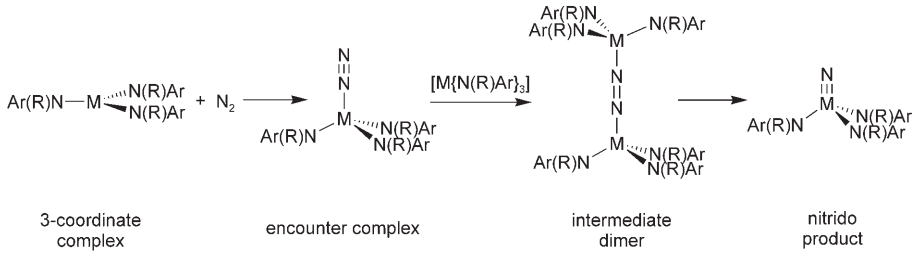


Scheme 1. Reaction mechanism for $N_2$ cleavage by $[Mo\{N(R)Ar\}_3]$.

The ability of $[Mo\{N(R)Ar\}_3]$ to break a bond of strength $D(N{\equiv}N) = (945.4 \pm 0.8)$ kJ mol$^{-1}$ derives, in part, from the formation of two nitrido complexes, each featuring a very strong Mo–N bond. Further assistance comes from the electronic properties of the reactant complex, which is able to channel electron density from the metal atom and its attendant ligands directly into the antibonding orbitals of the coordinated $N_2$.

These sterically hindered, coordinatively unsaturated transition-metal complexes are also known to coordinate other small molecules including $N_2$, $N_2O$, NO, CO, $CN^-$ and $NCO^-$, as well as elemental phosphorus, sulfur, tellurium and selenium.[24–29] Surprisingly, cleavage of the stronger N–NO bond of $N_2O$, in preference to the much weaker NN–O bond, has also been reported.[24,30] Further, quantum chemical calculations have established that the analogous tungsten complex $[W\{N(R)Ar\}_3]$ should be energetically better suited to dinitrogen cleavage than the molybdenum complex. If, as those theoretical studies suggest, other three-coordinate metal complexes are indeed superior to $[Mo\{N(R)Ar\}_3]$ in their nitrogen-splitting ability, then there is a strong possibility that these coordinatively versatile complexes may well be capable of breaking very strong bonds in other small molecules, including perhaps CO itself, by a mechanism analogous to that for $N_2$ cleavage. The present work examines this possibility.

Experimentally, there have been attempts to directly cleave the CO bond using three-coordinate metal complexes. In particular, the terminal carbide $[CMo\{N(R)Ar\}_3]^-$ has been prepared from $[OC{-}Mo\{N(R)Ar\}_3]$,[25,26] the latter being formed by reacting $[Mo\{N(R)Ar\}_3]$ with CO, but a second $[Mo\{N(R)Ar\}_3]$ complex does not bind to the oxygen terminus of CO to form a dimer and instead the oxygen atom is removed by other means. However, with different metals it may be possible to form the intermediate dimer $[\{Ar(R)N\}_3M{-}CO{-}M'\{N(R)Ar\}_3]$ and cleave CO in a similar manner to the cleavage of $N_2$ with $[Mo\{N(R)Ar\}_3]$. CO has been cleaved with $[Ta(silox)_3]$ ($silox = t$Bu$_3$SiO$^-$) to form $[O{=}Ta(silox)_3]$ and $[O{=}C{=}C{=}Ta(silox)_3]$ or $[(\mu\text{-}C_2)\{Ta(silox)_3\}_2]$.[31] Although some aspects of the mechanism remain unclear, it seems likely that the reaction proceeds through a mechanism involving a polynuclear $[OCTa(silox)_3]_n$ species rather than a $[(silox)_3Ta{-}CO{-}Ta(silox)_3]$ dimer intermediate. Cleavage of CO has also been reported with the ditungsten complex $[\{WCl(silox)_2\}_2]$, which reacts with CO to form the carbon-bridged dimer $[(silox)_2OW{=}C{=}WCl_2(silox)_2]$.[32]

To choose metals best suited to activating and cleaving CO, we turn to earlier work in which a systematic study of M–L bond strengths in model $[L{-}M(NH_2)_3]$ complexes (L = N, C and O), involving a wide range of metals, oxidation states and metal $d^n$ configurations, was conducted.[33] From this study the strongest M–N, M–O and M–C bonds were calculated for $d^3$, $d^2$ and $d^4$ metals, respectively, and for isoelectronic metals the bond energies were found to increase both down a group and to the left of a transition period. In principle, the results from this study allow the identification of metals that give the most stable products on cleavage of the small molecule $L^1{\equiv}L^2$, as shown in Scheme 2, on the basis that the

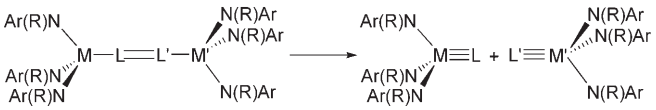


Scheme 2. The cleavage reaction of an heteronuclear diatomic molecule L≡L′.

formation of strong M–L bonds in the $[L{-}M(NH_2)_3]$ product is the thermodynamic driving force for the cleavage reaction. Furthermore, the factors that influence the strength of the M–L bond, such as M–L orbital overlap, also affect the degree of activation of the bound small molecule in the intermediate dimer $[(H_2N)_3M{-}L{-}L'{-}M'(NH_2)_3]$. The validity of this approach was tested by comparing both the extent of $N_2$ activation in the intermediate dimer and the barrier to $N_2$ bond cleavage with the calculated $[N{-}M(NH_2)_3]$ bond

  

energies. A strong correlation was shown to exist in that a concomitant increase in the calculated N–N bond length and a general trend towards lower activation barriers were observed with increasing M–N bond energy.

By assuming that the above approach applies to other diatomic molecules such as CO, we anticipate that metals that give the strongest $M-L^1$ and $M-L^2$ bonds will be the most suitable for binding and cleaving the small molecule $L^1{\equiv}L^2$. By using the results obtained from our earlier bond energy study, we predict that three-coordinate complexes involving $Re^{III}$ and $Ta^{III}$ will be best suited to cleaving the C–O bond, with $Re^{III}$ binding to carbon and $Ta^{III}$ to oxygen. With this choice of metals, the overall enthalpy for the model reaction [Eq. (1)] is calculated to be $-467\ kJ\,mol^{-1}$, which is considerably more exothermic than the $N_2$ cleavage reaction carried out with $[Mo(NH_2)_3]$ for which the reaction enthalpy is calculated to be $-335\ kJ\,mol^{-1}$. Accordingly, we now use density functional methods to explore in detail the reaction pathway for the cleavage of CO by the three-coordinate complexes $[Ta^{III}\{N(R)Ar\}_3]$ and $[Re^{III}\{N(R)Ar\}_3]$ with $NH_2$ used as a model for the bulky N(R)Ar ligands.

$$[Re^{III}(NH_2)_3] + [Ta^{III}(NH_2)_3] + CO \rightarrow [C{-}Re(NH_2)_3] + [O{-}Ta(NH_2)_3] \quad (1)$$

## Results and Discussion

Although the combination of the asymmetric diatomic CO and two different three-coordinate metal complexes can, in principle, lead to a number of possible reaction pathways, in this study we limit ourselves to metal-based reactions initiated by the terminal coordination of CO to the model complexes $[Re^{III}(NH_2)_3]$ or $[Ta^{III}(NH_2)_3]$.

In the first step, CO can react with either $[Re^{III}(NH_2)_3]$ or $[Ta^{III}(NH_2)_3]$ to form the encounter complexes $[OC{-}M^{III}(NH_2)_3]$ or $[CO{-}M^{III}(NH_2)_3]$ ($M = Re^{III}$ or $Ta^{III}$). Formation of the homonuclear $[(H_2N)_3M{\equiv}M(NH_2)_3]$ or heteronuclear $[(H_2N)_3M{\equiv}M'(NH_2)_3]$ metal–metal-bonded dimer can be excluded on steric grounds as the bulky R groups in the experimental N(R)Ar ligands prevent the metals from approaching close enough to form a metal–metal bond. Once formed, the encounter complex can potentially react with any remaining $[Re^{III}(NH_2)_3]$ or $[Ta^{III}(NH_2)_3]$ to form the intermediate dimer, $[(H_2N)_3M^{III}{-}CO{-}M'^{III}(NH_2)_3]$, with CO bridging end-on between the two metals. If favourable, the C–O bond will cleave to form the carbide $[C{-}M(NH_2)_3]$ and oxide $[O{-}M'(NH_2)_3]$ products.

In the following sections we will discuss the resulting structures and energetics for the different reaction pathways for the model system. We have previously calculated the structures of the reactants $[Re^{III}(NH_2)_3]$ and $[Ta^{III}(NH_2)_3]$ and the products $[C{-}Re(NH_2)_3]$ and $[O{-}Ta(NH_2)_3]$.[33] Consequently, the structural description that follows focuses on the possible encounter complexes $[OC{-}M^{III}(NH_2)_3]$ and $[CO{-}M^{III}(NH_2)_3]$ and intermediate dimer complexes $[(H_2N)_3M^{III}{-}CO{-}M'^{III}(NH_2)_3]$ arising from the different reactions.

**Formation of the encounter complex**: The reaction of carbon monoxide with $[Re^{III}(NH_2)_3]$ or $[Ta^{III}(NH_2)_3]$ leads to four possible encounter complexes, $[OC{-}Re^{III}(NH_2)_3]$, $[CO{-}Re^{III}(NH_2)_3]$, $[OC{-}Ta^{III}(NH_2)_3]$ and $[CO{-}Ta^{III}(NH_2)_3]$. Selected structural data calculated for all four complexes are given in Table 1 and the geometries of $[OC{-}Re^{III}(NH_2)_3]$ and $[OC{-}Ta^{III}(NH_2)_3]$ are shown in Figure 1.

Table 1. Selected geometrical parameters for the encounter complexes.

| Encounter complex | Bond lengths [Å] | | | Bond angles [°] | |
|---|---|---|---|---|---|
| | CO | M–C/M–O | M–N | C-M-N/O-M-N | M-C-O/M-O-C |
| $[OC{-}Re^{III}(NH_2)_3]$ | 1.190 | 1.807 | 1.937 | 97 | 180 |
| $[CO{-}Re^{III}(NH_2)_3]$ | 1.181 | 1.932 | 1.936 | 92 | 180 |
| $[OC{-}Ta^{III}(NH_2)_3]$ | 1.187 | 2.033 | 2.002, 1.993, 1.993 | 118, 103, 104 | 172 |
| $[CO{-}Ta^{III}(NH_2)_3]$ | 1.188 | 2.121 | 1.984, 1.996, 1.996 | 143, 88, 89 | 178 |

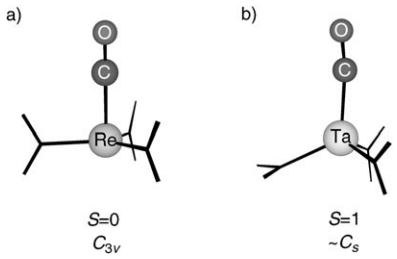


Figure 1. Optimized structures for a) $[OC{-}Re(NH_2)_3]$ and b) $[OC{-}Ta(NH_2)_3]$.

Both the carbon- and oxygen-bound encounter complexes of $Re^{III}$ are calculated to have $C_{3v}$ symmetry and spin singlet ground states, whereas those involving $Ta^{III}$ have spin triplet ground states and approximately $C_s$ symmetry, with one of the $NH_2$ ligands rotated by 90° around the $Ta{-}N_{amide}$ axis. The ligand rotation is the result of a Jahn–Teller distortion due to the single occupancy of the doubly degenerate HOMO involving the $d_{xz}$ and $d_{yz}$ orbitals on $Ta^{III}$. In addition to ligand rotation, a distinct bending of the CO group ($\sphericalangle$ Ta-C-O = 172°) is apparent in the structure of $[OC{-}Ta^{III}(NH_2)_3]$.

The calculated enthalpies for the possible reactions (2), (3), (4) and (5) are −277, 53, −153 and 6 kJ mol$^{-1}$, respectively.

$$[Re^{III}(NH_2)_3] + CO \rightarrow [OC{-}Re^{III}(NH_2)_3] \quad (2)$$

$$[Re^{III}(NH_2)_3] + CO \rightarrow [CO{-}Re^{III}(NH_2)_3] \quad (3)$$

  

$$[Ta^{III}(NH_2)_3] + CO \rightarrow [OC{-}Ta^{III}(NH_2)_3] \quad (4)$$

$$[Ta^{III}(NH_2)_3] + CO \rightarrow [CO{-}Ta^{III}(NH_2)_3] \quad (5)$$

The binding of CO through the carbon atom is clearly more favourable for both $Re^{III}$ and $Ta^{III}$ with the formation of $[OC{-}Re^{III}(NH_2)_3]$ the most exothermic reaction. The encounter complexes involving CO coordination through the oxygen atom are far less strongly bound as the reactions leading to $[CO{-}Re^{III}(NH_2)_3]$ and $[CO{-}Ta^{III}(NH_2)_3]$ are both endothermic. Based on the calculated enthalpies, the dominant encounter species are expected to be $[OC{-}Re^{III}(NH_2)_3]$ and $[OC{-}Ta^{III}(NH_2)_3]$.

The potential energy surfaces for the binding of CO to $[Re^{III}(NH_2)_3]$ and $[Ta^{III}(NH_2)_3]$ were explored further through linear transits in which the metal–carbon bond length was incremented and all other geometrical parameters were optimised. The results for $[OC{-}Re^{III}(NH_2)_3]$ and $[OC{-}Ta^{III}(NH_2)_3]$ are plotted in Figure 2. The linear transit results for the formation of $[CO{-}Re^{III}(NH_2)_3]$ and $[CO{-}Ta^{III}(NH_2)_3]$ are included in the Supporting Information.

With $[Re^{III}(NH_2)_3]$, the binding of CO initially occurs on the triplet surface but crosses over to the singlet for Re–C bond distances below 2.45 Å. There is no barrier to this step of the reaction in either spin state. The optimised singlet species is the ground state as it is 146 kJ mol$^{-1}$ lower in energy. With the $Ta^{III}$ complex, CO initially binds on the singlet surface, followed by spin crossover to the triplet. However, the singlet and triplet surfaces are similar in energy and, since spin–orbit coupling is significant for third-row transition metals, it is not possible to predict which is the true ground state. As found for $[OC{-}Re^{III}(NH_2)_3]$, there is no barrier to the formation of $[OC{-}Ta^{III}(NH_2)_3]$ in either spin state.

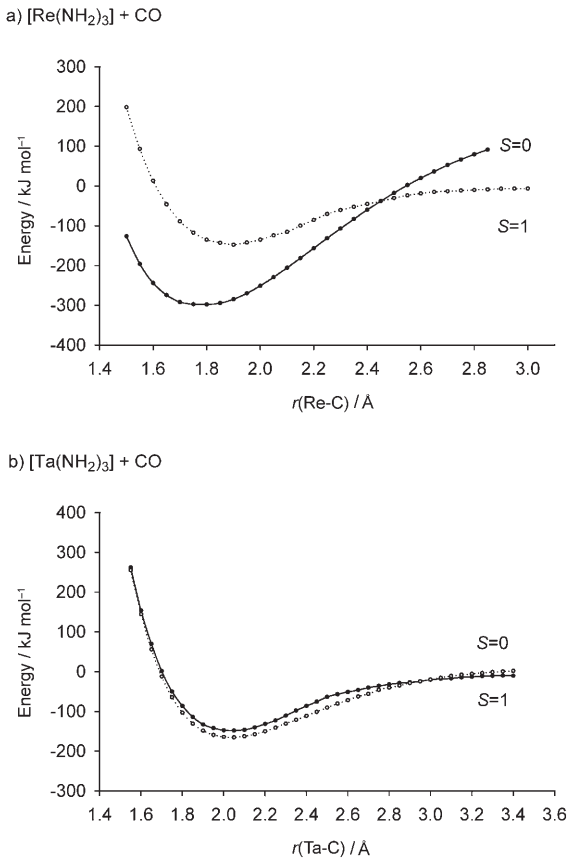


Figure 2. Linear transit results for the formation of the encounter complexes $[OC{-}M(NH_2)_3]$ ($M = Re^{III}$, $Ta^{III}$).

To place the exothermicity of $[OC{-}Re^{III}(NH_2)_3]$ and $[OC{-}Ta^{III}(NH_2)_3]$ formation in a wider context, it is useful to compare the present results with those obtained for the much-studied $N_2/[Mo(NH_2)_3]$ system.[21–23] The uptake of $N_2$ by $[Mo(NH_2)_3]$ to form $[N_2{-}Mo^{III}(NH_2)_3]$ is exothermic by only 71 kJ mol$^{-1}$ with a small barrier to formation.[34] In contrast, the uptake of CO by $[Mo(NH_2)_3]$ is calculated to be exothermic by 152 kJ mol$^{-1}$ with no barrier to formation.[34] On the basis of these calculations, we expect the formation of $[OC{-}Re^{III}(NH_2)_3]$, $[OC{-}Ta(NH_2)_3]$ and $[OC{-}Mo(NH_2)_3]$ to be more favourable than that of $[N_2{-}Mo^{III}(NH_2)_3]$. The greater stability calculated for the CO encounter complexes relative to their $N_2$ analogues is consistent with experimental observations in that $[OC{-}Mo\{N(tBu)Ar\}_3]$ has been isolated whereas $[N_2{-}Mo\{N(R)Ar\}_3]$ has not yet been observed.[19,20]

**Formation of the intermediate dimer and products**: In the Re/Ta reaction, there are two dominant encounter complexes, $[OC{-}Re^{III}(NH_2)_3]$ and $[OC{-}Ta^{III}(NH_2)_3]$. As either complex can react with excess $[Re^{III}(NH_2)]$ or $[Ta^{III}(NH_2)_3]$, then in principle four intermediate dimer species can form. The main geometrical parameters calculated for the lowest energy structure of each dimer are listed in Table 2 and the structures of $[(H_2N)_3Re^{III}{-}CO{-}Ta^{III}(NH_2)_3]$, $[(H_2N)_3Re^{III}{-}CO{-}Re^{III}(NH_2)_3]$, $[(H_2N)_3Ta^{III}{-}CO{-}Re^{III}(NH_2)_3]$ and $[(H_2N)_3Ta^{III}{-}CO{-}Ta^{III}(NH_2)_3]$ are shown in Figure 3.

Except for $[(H_2N)_3Re^{III}{-}CO{-}Ta^{III}(NH_2)_3]$, all dimers are calculated to have singlet ground states and elongated C–O bonds in the range of 1.21–1.31 Å (cf. 1.128 Å in free CO), indicating significant C–O bond activation. Ligand rotation, similar to that observed in the $[OC{-}Ta(NH_2)_3]$ encounter complex, is also present in the optimised structures of $[(H_2N)_3Re^{III}{-}CO{-}Re^{III}(NH_2)_3]$ and $[(H_2N)_3Ta^{III}{-}CO{-}Ta^{III}(NH_2)_3]$, as can be seen from Figure 3. The $[(H_2N)_3Re^{III}{-}CO{-}Re^{III}(NH_2)_3]$ dimer has a local trigonal axis at the rhenium centre bound to the carbon atom, but one amide ligand on the other rhenium centre is rotated by 90°. The $[(H_2N)_3Ta^{III}{-}CO{-}Ta^{III}(NH_2)_3]$ structure has one amide ligand rotated at both metal centres and exhibits the most elongated CO bond (1.306 Å). The $[(H_2N)_3Ta^{III}{-}CO{-}Re^{III}(NH_2)_3]$ dimer also has one ligand rotated at the tantalum centre, but the coordination around the rhenium centre is very different, with all three ligands lying approximately in one plane giving rise to a pseudo-square-planar arrangement if the CO ligand is included.

In contrast to the above singlet dimer structures, optimisation of $[(H_2N)_3Re^{III}{-}CO{-}Ta^{III}(NH_2)_3]$ in the singlet spin state results in spontaneous scission of the C–O bond indi-

  

Table 2. Selected geometrical parameters for the intermediate dimers.

| Intermediate dimer | Bond lengths [Å] | | | | Bond angles [°] | |
|---|---|---|---|---|---|---|
| | C–O | M–C | M–O | M–N (av) | M-C-O | M-O-C |
| $[(H_2N)_3Re^{III}–CO–Re^{III}(NH_2)_3]$ | 1.213 | 1.803 | 2.120 | 1.925 | 173 | 157 |
| $[(H_2N)_3Re^{III}–CO–Ta^{III}(NH_2)_3]$ | 1.350 | 1.807 | 1.950 | 1.954 | 140 | 135 |
| $[(H_2N)_3Ta^{III}–CO–Re^{III}(NH_2)_3]$ | 1.248 | 1.933 | 1.877 | 1.971 | 174 | 179 |
| $[(H_2N)_3Ta^{III}–CO–Ta^{III}(NH_2)_3]$ | 1.306 | 1.894 | 1.854 | 2.000 | 168 | 170 |

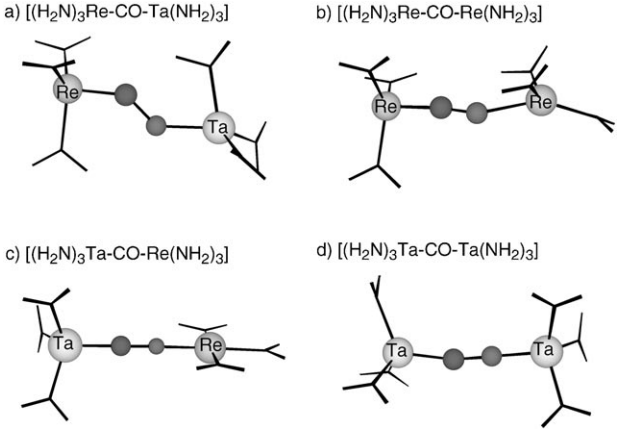


Figure 3. Optimised structures for the intermediate dimers $[(H_2N)_3M–CO–M'(NH_2)_3]$ (M, M′ = $Re^{III}$, $Ta^{III}$).

cating that the barrier to C–O bond cleavage is small or non-existent for this complex. The structure of this dimer (with a fixed CO bond length of 1.350 Å), shown in Figure 3, reveals that the ligand arrangement around the $Re^{III}$ centre is trigonal, but the coordination around the $Ta^{III}$ centre is quite distorted with two ligands rotated. A triplet-state structure for this dimer exists with a CO bond distance of 1.241 Å, but it is at least 20 kJ mol$^{-1}$ higher in energy than the singlet. The reaction profile involving this dimer is discussed in more detail in the following section.

Consideration of all four dimers leads to the formation of four possible products, $[C–Re(NH_2)_3]$, $[O–Re(NH_2)_3]$, $[C–Ta(NH_2)_3]$ or $[O–Ta(NH_2)_3]$, on cleavage of the C–O bond. We have previously calculated the structures and energies of $[C–Re(NH_2)_3]$ and $[O–Ta(NH_2)_3]$.[33] Singlet ground states were obtained for $[C–Re(NH_2)_3]$, $[O–Re(NH_2)_3]$ and $[O–Ta(NH_2)_3]$, whereas $[C–Ta(NH_2)_3]$ was found to have a triplet ground state. Both $[C–Re(NH_2)_3]$ and $[O–Ta(NH_2)_3]$ were shown to have trigonal symmetry, whereas $[O–Re(NH_2)_3]$ has $C_s$ symmetry with one ligand rotated and $[C–Ta(NH_2)_3]$ has no symmetry and two ligands rotated.

The calculated energies of the encounter complex, $[OC–M(NH_2)_3]$, intermediate dimer, $[(H_2N)_3M–CO–M'(NH_2)_3]$, and CO cleavage products, $[CM(NH_2)_3]+[OM'(NH_2)_3]$, for M and M′ = $Re^{III}$ or $Ta^{III}$ relative to the energy of the reactants, $[M(NH_2)_3]+CO+[M'(NH_2)_3]$, are summarised in Table 3 for the four possible reactions.

For each reaction, the intermediate dimer is calculated to be more stable than the relevant encounter complex with the exception of $[(H_2N)_3Re^{III}–CO–Re^{III}(NH_2)_3]$ which is approximately 215 and 150 kJ mol$^{-1}$, respectively, less stable than the intermediate dimer. Thus, for these two dimers, C–O bond cleavage is unlikely. Interestingly, both these cleavage reactions require the formation of the $[OC–Ta^{III}(NH_2)_3]$ encounter complex, whereas the reactions involving the more strongly bound $[OC–Re^{III}(NH_2)_3]$ encounter complex have exothermic CO cleavage steps.

Table 3. Calculated energies of the encounter complex, intermediate dimer and products relative to the reactants for the reaction $[M^{III}(NH_2)_3]+CO+[M'^{III}(NH_2)_3]\rightarrow[OC–M^{III}(NH_2)_3]+[M'^{III}(NH_2)_3]\rightarrow[(H_2N)_3M^{III}–CO–M'^{III}(NH_2)_3]\rightarrow[C–M(NH_2)_3]+[O–M'(NH_2)_3]$.

| Reaction | M | M′ | Energy [kJ mol$^{-1}$] | | |
|---|---|---|---|---|---|
| | | | En. complex M–CO | Dimer M-CO-M′ | Products M–C+O–M′ |
| 6 | $Re^{III}$ | $Re^{III}$ | −277 | −256 | −301 |
| 7 | $Re^{III}$ | $Ta^{III}$ | −277 | −316[a] | −467 |
| 8 | $Ta^{III}$ | $Re^{III}$ | −153 | −237 | −23 |
| 9 | $Ta^{III}$ | $Ta^{III}$ | −153 | −340 | −189 |

[a] C–O bond fixed at 1.350 Å as dimer undergoes spontaneous cleavage of the CO bond.

The energetic differences between the various reaction pathways can be rationalised by considering the number of d electrons on the metals and the stability of the products. For $[(H_2N)_3Ta^{III}–CO–Ta^{III}(NH_2)_3]$ there is a total of four d electrons on the metals which is two short of the six necessary to fill the σ* and π* orbitals of CO and thus reductively cleave the CO bond. Cleavage of the C–O bond in this dimer is therefore unfavourable. For $[(H_2N)_3Ta^{III}–CO–Re^{III}(NH_2)_3]$ there are six d electrons available to fill the CO antibonding orbitals, but the $Ta^{III}$–C and $Re^{III}$–O bonds are relatively weak as $Ta^{III}(d^2)$ and $Re^{III}(d^4)$ do not have the optimum $d^n$ configurations to bind strongly to the carbon and oxygen atoms, respectively, and consequently the products are not very stable.[33] In the case of $[(H_2N)_3Re^{III}–CO–Re^{III}(NH_2)_3]$ there are two $d^4$ metal centres so there are excess electrons to reductively cleave the CO bond. However, for a $d^4$ metal, two of the d electrons in $[O–M'^{III}(NH_2)_3]$ occupy M–O antibonding orbitals and thus destabilize the products. Analogous to $[(H_2N)_3Ta^{III}–CO–Re^{III}(NH_2)_3]$, the reaction involving $[(H_2N)_3Re^{III}–CO–Ta^{III}(NH_2)_3]$ also has the necessary six d electrons on the metals, but in this case $Re^{III}(d^4)$ and $Ta^{III}(d^2)$ have the optimum $d^n$ configurations necessary to strongly bind carbon and oxygen atoms, respectively, resulting in greater stabilization of the products.

The importance of the correct $d^n$ configuration on the metal atom is further highlighted in the case of the $[Mo\{N(R)Ar\}_3]+CO$ reaction. Experimentally, although the encounter complex $[OC–Mo\{N(tBu)Ar\}_3]$ has been isolated,

  

the reaction does not progress beyond this point and, consequently, CO bond cleavage is not observed.[25,26] This result can be rationalised on the basis that although $[(H_2N)_3Mo^{III}–CO–Mo^{III}(NH_2)_3]$ is isoelectronic with $[(H_2N)_3Mo^{III}–N_2–Mo^{III}(NH_2)_3]$ and therefore has the required number of electrons to cleave CO, $Mo^{III}$ does not have the optimum $d^n$ configuration to form strong M–C and M–O bonds to sufficiently stabilize the products.[33]

**Cleavage of the C–O bond**: On the basis of the data in Table 3, reactions (6) and (7) are both thermodynamically favourable but this conclusion ignores any kinetic barriers to the formation of the intermediate dimers or cleavage of the C–O bond. To examine the reaction profile in more detail and to obtain a measure of any kinetic barriers to M–CO bond formation and C–O cleavage, linear transits were performed on the intermediate dimers $[(H_2N)_3Re^{III}–CO–Re^{III}(NH_2)_3]$ and $[(H_2N)_3Re^{III}–CO–Ta^{III}(NH_2)_3]$. Linear transits were not undertaken for the dimer species involved in reactions (8) and (9) because in both cases the intermediate dimer is the lowest energy species on the reaction pathway and therefore cleavage of the C–O bond is energetically unfavourable.

The linear transit data for reaction (6), involving the binding of $[Re^{III}(NH_2)_3]$ end-on to $[OC–Re^{III}(NH_2)_3]$ and the cleavage of the CO bond in the dimer, are included in the Supporting Information. From this data, the barriers to the formation of the intermediate dimer and cleavage of the CO bond are approximately 30 and 93 kJ mol$^{-1}$, respectively. As the barrier to CO cleavage is significant and the overall cleavage step is exothermic by 45 kJ mol$^{-1}$, the $Re^{III}$/CO/$Re^{III}$ system is clearly inferior to the $Re^{III}$/CO/$Ta^{III}$ system discussed below and will be considered no further.

The linear transit curves for the formation of $[(H_2N)_3Re^{III}–CO–Ta^{III}(NH_2)_3]$ as a function of the $\{O–Ta^{III}(NH_2)_3\}$ bond distance are shown in Figure 4a. The initial approach of $[OC–Re^{III}(NH_2)_3]$ and $[Ta^{III}(NH_2)_3]$ to form the intermediate dimer occurs on the singlet surface. For intermediate Ta–O distances between 3.0 and 2.2 Å, the triplet is the ground state, but below 2.2 Å the singlet crosses the triplet surface again and is lower in energy. As the Ta–O distance falls below 2.2 Å, the C–O bond cleaves and the energy drops sharply by over 100 kJ mol$^{-1}$. The dramatic drop in energy and lack of a minimum for the $[(H_2N)_3Re^{III}–CO–Ta^{III}(NH_2)_3]$ dimer on the singlet surface indicates a low barrier to C–O cleavage for this system. The barrier to forming the intermediate dimer is approximately 20 kJ mol$^{-1}$ if the system remains in the singlet state. However, given that spin–orbit coupling is not insignificant for either $Re^{III}$ and $Ta^{III}$, this barrier is likely to be even smaller.

The linear transit results for C–O bond cleavage in $[(H_2N)_3Re^{III}–CO–Ta^{III}(NH_2)_3]$ are shown in Figure 4b. For the singlet surface, a smooth decrease in energy is observed as the C–O bond length increases and consequently there is no barrier to C–O bond cleavage in this spin state. The triplet surface exhibits a minimum for the dimer at approximately 1.25 Å but this minimum is at a higher energy than the singlet curve except at unrealistically small C–O bond lengths.

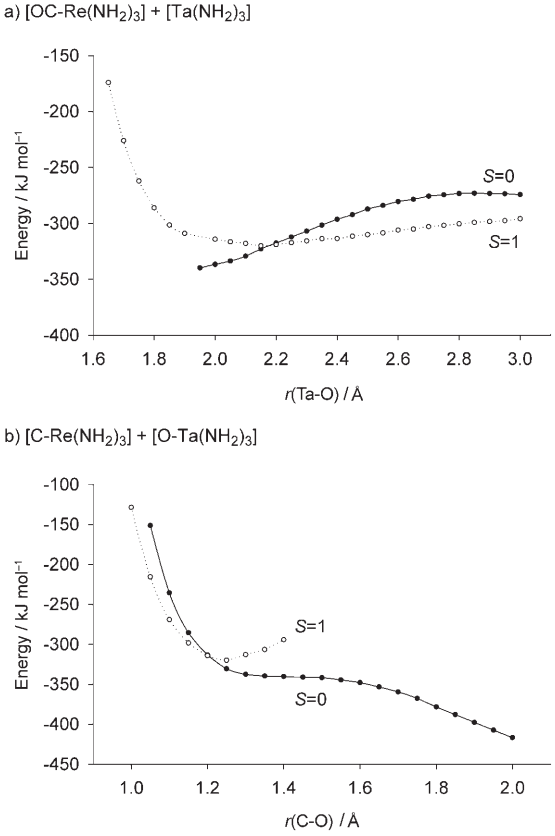


Figure 4. Linear transit results for the formation of the intermediate dimer $[(H_2N)_3Re–CO–Ta(NH_2)_3]$ and cleavage of the C–O bond. a) $[OC–Re(NH_2)_3]+[Ta(NH_2)_3]\rightarrow[(H_2N)_3Re–CO–Ta(NH_2)_3]$. b) $[(H_2N)_3Re–CO–Ta(NH_2)_3]\rightarrow[C–Re(NH_2)_3]+[O–Ta(NH_2)_3]$. Energies are given relative to the reactants.

The overall reaction profile showing the relative energies of the reactants, encounter complex, intermediate dimer and products for the $[Re(NH_2)_3]$/CO/$[Ta(NH_2)_3]$ reaction is plotted in Figure 5. The approximate minimum-energy crossing point for the encounter complex to intermediate dimer step is also included. On the basis of Figure 2 through to Figure 5, the main reaction proceeds as follows: CO binds to triplet $[Re^{III}(NH_2)_3]$ without a barrier and is followed by spin crossover to form the singlet encounter complex $[OC–Re^{III}(NH_2)_3]$, which is stabilized by 277 kJ mol$^{-1}$ relative to the reactants. This is followed by the binding of $[Ta^{III}(NH_2)_3]$ on the singlet surface to the oxygen terminus of CO with a barrier of approximately 20 kJ mol$^{-1}$. Spontaneous cleavage of the C–O bond then occurs to form the singlet products $[C–Re(NH_2)_3]$ and $[O–Ta(NH_2)_3]$ which are stabilized by 190 kJ mol$^{-1}$ relative to the encounter complex. The low barrier calculated for this pathway indicates that the reaction of CO with $[Re^{III}(NH_2)_3]$ and $[Ta^{III}(NH_2)_3]$ should proceed quickly. Given the large exothermicity and low barrier, the reaction should be favourable for second-row transition metals such as $Nb^{III}$ and $Tc^{III}$ as well.

  

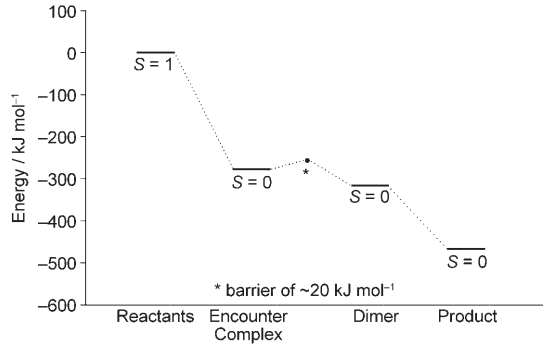


Figure 5. Overall reaction profile for the cleavage of CO by $[Re^{III}(NH_2)_3]$ and $[Ta^{III}(NH_2)_3]$ through the reaction $[Re^{III}(NH_2)_3]+CO+[Ta^{III}(NH_2)_3]\rightarrow[OC{-}Re^{III}(NH_2)_3]+[Ta^{III}(NH_2)_3]\rightarrow[(H_2N)_3Re^{III}{-}CO{-}Ta^{III}(NH_2)_3]\rightarrow[C{-}Re^{III}(NH_2)_3]+[O{-}Ta^{III}(NH_2)_3]$. Energies shown are relative to the reactants. The barrier of 20 kJ mol$^{-1}$ to the formation of the dimer is included.

In the model calculations discussed above, the symmetry of the $\{M(NH_2)_3\}$ fragment was not constrained. However, in the experimental system, the size of the N(R)Ar ligands may limit any distortion from an approximately trigonal arrangement around the metal centre and thus affect the overall reaction energetics. For example, in a previous study of the deoxygenation of $R_3PO$ and $[ON{-}W(silox)_3]$ by $[M(silox)_3]$ (M = V, Nb and Ta), steric factors were found to play an important role in the size of the barrier to N–O and P–O cleavage.[35] Calculations showed that the barrier to deoxygenation of $Ph_3PO$ was considerably greater when the M–O–E geometry (E = $Ph_3P$ or $[NW(silox)_3]$) was constrained to be linear.

To examine the effects of symmetry constraints on the reaction energetics, the formation of $[(H_2N)_3Re^{III}{-}CO{-}Ta^{III}(NH_2)_3]$ and subsequent cleavage of the CO bond were investigated with $C_3$ symmetry and a linear Re-CO-Ta core. From these calculations, the barrier to dimer formation was estimated to be 31 and 45 kJ mol$^{-1}$ for the triplet and singlet states, respectively, compared with 12 and 25 kJ mol$^{-1}$ for the unconstrained calculations. Thus, symmetry constraints only result in an increase in the barrier to dimer formation of around 20 kJ mol$^{-1}$. The barrier to CO cleavage exhibits a greater dependence on symmetry constraints. In the unconstrained case there is no barrier to CO cleavage, but when $C_3$ symmetry is enforced, the barrier to C–O cleavage is calculated to be 35 kJ mol$^{-1}$ and, in contrast to the unconstrained calculations, the intermediate dimer has a triplet ground state.

Although trigonal ($C_3$) symmetry constraints impose a moderate barrier to CO cleavage, previous calculations on $[N_2{-}(Mo\{N(t\text{Bu})Ar\}_3)_2]$ have shown that the bulky N(*t*Bu)Ar ligands are free to rotate away from the $C_3$ symmetry and that the Mo-N-N-Mo core is still able to bend slightly.[36] Since the $[\{Ar(t\text{Bu})N\}_3Re{-}CO{-}Ta\{N(t\text{Bu})Ar\}_3]$ structure should have similar flexibility, the $C_3$ barrier can be considered the "worst case scenario".

The effects of the full ligands on the reaction enthalpy have been studied by using QM/MM methods for the cleavage of $N_2$ by $[Mo\{N(t\text{Bu})Ar\}_3]$[34] and the cleavage of the N–N bond in $N_2O$ by $[Mo\{N(t\text{Bu})Ar\}_3]$.[37] In all three cases, the reaction enthalpy was found to decrease by 30–40 kJ mol$^{-1}$ when the full ligands were included and the activation barrier to N–N cleavage by $[Mo\{N(t\text{Bu})Ar\}_3]$ showed an increase of 36 kJ mol$^{-1}$.[34] Based on these results and the fact that the calculated barrier to CO cleavage in the model system is less than the calculated value for the cleavage of $N_2$ by $[Mo^{III}(NH_2)_3]$, we expect that CO cleavage should be facile at room temperature for the real system.

**CO activation without cleavage**: There is considerable interest in the possible application of three-coordinate complexes as catalysts for small molecule activation. Consequently, as with the $N_2$ cleavage reaction, it may be advantageous to weaken the C–O bond while bound in the intermediate dimer but not to cleave it. This approach would allow chemistry to be performed directly on activated CO rather than on the strongly bound carbide and oxide cleavage products that essentially act as a thermodynamic sink preventing regeneration of the reactants in any catalytic process. The $d^3d^2$ dimeric complex $[\{Ar(R)N\}_3Mo(\mu\text{-}N_2)Nb\{N(R)Ar\}_3]$, which has been structurally characterized[38] and its $N_2$ cleavage reaction investigated by density functional methods,[39] serves as a useful prototype in this context. This complex exhibits a significantly activated N–N bond of 1.235 Å (cf. 1.105 Å in free $N_2$), but does not undergo $N_2$ cleavage as it is one electron short of the six electrons necessary for the full reductive cleavage of dinitrogen.

Applying the above approach to CO activation requires the replacement of either the $d^4$ $Re^{III}$ centre bound to the carbon atom with a $d^3$ metal such as $Mo^{III}$ or $W^{III}$, or the replacement of the $d^2$ $Ta^{III}$ centre bound to the oxygen atom with a $d^1$ metal such as $Nb^{III}$ or $Hf^{III}$. However, on the basis of previous work,[33] the M–O bond energies exhibit greater variation with $d^n$ configuration than the M–C bond energies and therefore it is preferable to replace $Re^{III}$ with $W^{III}$ and thus investigate the intermediate dimer $[(H_2N)_3W^{III}{-}CO{-}Ta^{III}(NH_2)_3]$. Calculations on $[(H_2N)_3W^{III}{-}CO{-}Ta^{III}(NH_2)_3]$ show that this complex does indeed possess a significantly activated C–O bond of 1.311 Å (cf. 1.128 Å in free CO), even greater than the CO bond of 1.306 Å in the ditantalum(III) dimer. Furthermore, the actual cleavage step to form the $[C{-}W(NH_2)_3]$ and $[O{-}Ta(NH_2)_3]$ products is calculated to be endothermic by over 68 kJ mol$^{-1}$. Thus, at lower temperatures, at which the barrier to CO cleavage is unlikely to be overcome, this complex seems well suited to performing activated CO chemistry.

## Conclusion

Our analysis of the reaction involving $[Re(NH_2)_3]$, $[Ta(NH_2)_3]$ and CO shows that only two pathways are viable thermodynamically. For the reaction involving $[(H_2N)_3Re^{III}{-}CO{-}Re^{III}(NH_2)_3]$, a barrier of approximately 30 kJ mol$^{-1}$ inhibits the formation of the intermediate dimer from [OC–

  

$Re^{III}(NH_2)_3$] and [$Re^{III}(NH_2)_3$], and an even larger barrier of 93 kJ mol$^{-1}$ impedes cleavage of the C–O bond once the dimer is formed. Although these barriers are not insurmountable, the second reaction involving the formation of [$(H_2N)_3Re^{III}$–CO–$Ta^{III}(NH_2)_3$] from [OC–$Re^{III}(NH_2)_3$] and [$Ta^{III}(NH_2)_3$] has a maximum barrier of only 20 kJ mol$^{-1}$ and the CO cleavage step is barrierless. Furthermore, the overall reaction is more exothermic by over 160 kJ mol$^{-1}$. Consequently, we anticipate that the reaction involving the formation of [$(H_2N)_3Re^{III}$–CO–$Ta^{III}(NH_2)_3$] will be the more significant pathway. Although other reactions involving the binding of CO to [$Ta^{III}(NH_2)_3$] to form [OC–$Ta^{III}(NH_2)_3$] are not capable of cleaving CO, they do lead to the formation of stable dimer species. However, it should be possible to minimise the formation of these complexes by controlling the reaction conditions, for example, by adding [$Ta^{III}(NH_2)_3$] after the formation of [OC–$Re^{III}(NH_2)_3$].

In contrast to the above CO cleavage reaction involving [$(H_2N)_3Re^{III}$–CO–$Ta^{III}(NH_2)_3$], the analogous cleavage of $N_2$ by [$Mo^{III}(NH_2)_3$] has a significantly higher cleavage barrier of 66 kJ mol$^{-1}$ and the overall reaction is less exothermic by 132 kJ mol$^{-1}$.[23] The cleavage of CO by [$Re^{III}(NH_2)_3$] and [$Ta^{III}(NH_2)_3$] is therefore considerably more favourable from both a thermodynamic and a kinetic viewpoint. Given that the cleavage of $N_2$ by three-coordinate [Mo{N(R)Ar}$_3$] has been observed experimentally,[19,40] we anticipate that the CO cleavage reaction described above will proceed even more rapidly.

## Computational Details

The calculations carried out in this work were performed using the Amsterdam Density Functional (ADF)[41–43] program (2002.03 and 2004 versions) running on either Linux-based Pentium IV computers or the Australian National University Supercomputing Facility. All calculations were performed using the local density approximation (LDA) to the exchange potential, the correlation potential of Vosko, Wilk and Nusair (VWN),[44] the Becke[45] and Perdew[46] corrections for non-local exchange and correlation, and the numerical integration scheme of te Velde and Baerends.[47] Geometry optimisations were performed using the gradient algorithm of Versluis and Ziegler.[48] All electron, triple-$\zeta$ Slater-type orbital basis sets (TZP) with polarisation functions were used for all atoms. All calculations were carried out in a spin-unrestricted manner. Relativistic effects were incorporated using the zero-order relativistic approximation (ZORA).[49–51] Minima were confirmed by the absence of any imaginary frequencies, the latter being computed by numerical differentiation of energy gradients in slightly displaced geometries. The energies of optimised structures were corrected for zero-point vibrational energy. The convergence criteria for geometry optimisations were $10^{-3}$ hartrees for energy and $10^{-2}$ hartrees Å$^{-1}$ for gradient. SCF convergence was set at $10^{-6}$. The integration parameter, accint, was set to 4.0 for geometry optimisations and to 6.0 for frequency calculations.

## Acknowledgements

The authors gratefully acknowledge the Australian Research Council for financial support in the form of an Australian Postgraduate Award for G.C. and a Discovery Project Grant for R.S. and B.F.Y. The National Science Foundation of the USA is acknowledged for funding support (CHE-0316823) to C.C.C. The Australian National University is also acknowledged for providing access to the APAC (Australian Partnership for Advanced Computing) supercomputing facilities.

[1] C. A. Piantadosi, *Antioxid. Redox Signaling* **2002**, *4*, 259–270.
[2] S. W. Ryter, L. E. Otterbein, *BioEssays* **2004**, *26*, 270–280.
[3] L. Wu, R. Wang, *Pharmacol. Rev.* **2005**, *57*, 585–630.
[4] H. P. Kim, S. W. Ryter, A. M. K. Choi, *Annu. Rev. Pharmacol. Toxicol.* **2006**, *46*, 411–449.
[5] S. Ragsdale, *Crit. Rev. Biochem. Mol. Biol.* **2004**, *39*, 165–195.
[6] P. C. Ford, *Electrochem. Electrocatal. React. Carbon Dioxide* **1993**, 68–93.
[7] A. A. Adesina, *Appl. Catal. A* **1996**, *138*, 345–367.
[8] H. Schulz, *Appl. Catal. A* **1999**, *186*, 3–12.
[9] P. M. Maitlis, *J. Organomet. Chem.* **2004**, *689*, 4366–4374.
[10] H. Papp, M. Baerns, *Stud. Surf. Sci. Catal.* **1991**, *64*, 430–461.
[11] V. Macho, M. Kralik, L. Komora, *Pet. Coal* **1997**, *39*, 6–12.
[12] J. R. Postgate, *Nitrogen Fixation*, Cambridge University Press, Cambridge, **1998**.
[13] J. R. Jennings, *Catalytic Ammonia Synthesis. Fundamentals and Practice, Vol. 1*, Plenum Press, New York, **1991**.
[14] M. D. Fryzuk, S. A. Johnson, *Coord. Chem. Rev.* **2000**, *200–202*, 379–409.
[15] M. Hidai, *Coord. Chem. Rev.* **1999**, *186*, 99–108.
[16] J. B. Howard, D. C. Rees, *Chem. Rev.* **1996**, *96*, 2965–2982.
[17] B. A. MacKay, M. D. Fryzuk, *Chem. Rev.* **2004**, *104*, 385–401.
[18] M. P. Shaver, M. D. Fryzuk, *Adv. Synth. Catal.* **2003**, *345*, 1061–1076.
[19] C. E. Laplaza, M. J. A. Johnson, J. C. Peters, A. L. Odom, E. Kim, C. C. Cummins, G. N. George, I. J. Pickering, *J. Am. Chem. Soc.* **1996**, *118*, 8623–8638.
[20] J. C. Peters, J. P. F. Cherry, J. C. Thomas, L. Baraldo, D. J. Mindiola, W. M. Davis, C. C. Cummins, *J. Am. Chem. Soc.* **1999**, *121*, 10053–10067.
[21] Q. Cui, D. G. Musaev, M. Svensson, S. Sieber, K. Morokuma, *J. Am. Chem. Soc.* **1995**, *117*, 12366–12367.
[22] K. M. Neyman, V. A. Nasluzov, J. Hahn, C. R. Landis, N. Rösch, *Organometallics* **1997**, *16*, 995–1000.
[23] G. Christian, J. Driver, R. Stranger, *Faraday Discuss.* **2003**, *124*, 331–341.
[24] C. E. Laplaza, A. L. Odom, W. M. Davis, C. C. Cummins, J. D. Protasiewicz, *J. Am. Chem. Soc.* **1995**, *117*, 4999–5000.
[25] J. C. Peters, A. L. Odom, C. C. Cummins, *Chem. Commun.* **1997**, 1995–1996.
[26] J. B. Greco, J. C. Peters, T. A. Baker, W. M. Davis, C. C. Cummins, G. Wu, *J. Am. Chem. Soc.* **2001**, *123*, 5003–5013.
[27] M. G. Fickes, A. L. Odom, C. C. Cummins, *Chem. Commun.* **1997**, 1993–1994.
[28] J. C. Peters, L. M. Baraldo, T. A. Baker, A. R. Johnson, C. C. Cummins, *J. Organomet. Chem.* **1999**, *591*, 24–35.
[29] C. C. Cummins, *Chem. Commun.* **1998**, 1777–1786.
[30] J.-P. F. Cherry, A. R. Johnson, L. M. Baraldo, Y.-C. Tsai, C. C. Cummins, S. V. Kryatov, E. V. Rybak-Akimova, K. B. Capps, C. D. Hoff, C. M. Haar, S. P. Nolan, *J. Am. Chem. Soc.* **2001**, *123*, 7271–7286.
[31] D. R. Neithamer, R. E. Lapointe, R. A. Wheeler, D. S. Richeson, G. D. Vanduyne, P. T. Wolczanski, *J. Am. Chem. Soc.* **1989**, *111*, 9056–9072.
[32] R. L. Miller, P. T. Wolczanski, A. L. Rheingold, *J. Am. Chem. Soc.* **1993**, *115*, 10422–10423.
[33] G. Christian, R. Stranger, B. F. Yates, *Inorg. Chem.* **2006**, *45*, 6851–6859.
[34] G. Christian, R. Stranger, unpublished results.
[35] A. S. Veige, L. M. Slaughter, E. B. Lobkovsky, P. T. Wolczanski, N. Matsunaga, S. A. Decker, T. R. Cundari, *Inorg. Chem.* **2003**, *42*, 6204–6224.
[36] G. Christian, R. Stranger, B. F. Yates, D. C. Graham, *Dalton Trans.* **2005**, 962–968.

  

[37] D. V. Khoroshun, D. G. Musaev, K. Morokuma, *Organometallics* **1999**, *18*, 5653–5660.
[38] D. J. Mindiola, K. Meyer, J.-P. F. Cherry, T. A. Baker, C. C. Cummins, *Organometallics* **2000**, *19*, 1622–1624.
[39] G. Christian, R. Stranger, *Dalton Trans.* **2004**, 2492–2495.
[40] C. E. Laplaza, C. C. Cummins, *Science* **1995**, *268*, 861–863.
[41] G. te Velde, F. M. Bickelhaupt, E. J. Baerends, C. Fonseca Guerra, S. J. A. Van Gisbergen, J. G. Snijders, T. Ziegler, *J. Comput. Chem.* **2001**, *22*, 931–967.
[42] C. Fonseca Guerra, J. G. Snijders, G. te Velde, E. J. Baerends, *Theor. Chem. Acc.* **1998**, *99*, 391–403.
[43] Theoretical chemistry software: Amsterdam Density Functional (ADF), versions 2002.03 and 2004, E. J. Baerends, J. Autschbach, A. Bérces, F. M. Bickelhaupt, C. Bo, P. M. Boerrigter, L. Cavallo, D. P. Chong, L. Deng, R. M. Dickson, D. E. Ellis, M. van Faassen, L. Fan, T. H. Fischer, C. Fonseca Guerra, S. J. A. van Gisbergen, J. A. Groeneveld, O. V. Gritsenko, M. Grüning, F. E. Harris, P. van den Hoek, C. R. Jacob, H. Jacobsen, L. Jensen, G. van Kessel, F. Kootstra, E. van Lenthe, D. A. McCormack, A. Michalak, J. Neugebauer, V. P. Osinga, S. Patchkovskii, P. H. T. Philipsen, D. Post, C. C. Pye, W. Ravenek, P. Ros, P. R. T. Schipper, G. Schreckenbach, J. G. Snijders, M. Solà, M. Swart, D. Swerhone, G. te Velde, P. Vernooijs, L. Versluis, L. Visscher, O. Visser, F. Wang, T. A. Wesolowski, E. van Wezenbeek, G. Wiesenekker, S. K. Wolff, T. K. Woo, A. L. Yakovlev, T. Ziegler, SCM, Theoretical Chemistry, Vrije Universiteit, Amsterdam, (The Netherlands), http://www.scm.com, **2002**.
[44] S. H. Vosko, L. Wilk, M. Nusair, *Can. J. Phys.* **1980**, *58*, 1200–1211.
[45] A. D. Becke, *Phys. Rev. A* **1988**, *38*, 3098–3100.
[46] J. P. Perdew, *Phys. Rev. B* **1986**, *33*, 8822–8824.
[47] G. te Velde, E. J. Baerends, *J. Comput. Phys.* **1992**, *99*, 84–98.
[48] L. Versluis, T. Ziegler, *J. Chem. Phys.* **1988**, *88*, 322–328.
[49] E. van Lenthe, E. J. Baerends, J. G. Snijders, *J. Chem. Phys.* **1993**, *99*, 4597–4610.
[50] E. van Lenthe, E. J. Baerends, J. G. Snijders, *J. Chem. Phys.* **1994**, *101*, 9783–9792.
[51] E. van Lenthe, A. Ehlers, E. J. Baerends, *J. Chem. Phys.* **1999**, *110*, 8943–8953.

Received: November 16, 2006
Published online: March 27, 2007

  